

Type-I-like intermittent chaos in multicomponent plasmas with negative ions

D. L. Feng, J. Zheng, W. Huang, and C. X. Yu

Department of Modern Physics, University of Science and Technology of China, Hefei, Anhui 230026, People's Republic of China

W. X. Ding

Chinese Center of Advanced Science and Technology (World Laboratory), P.O. Box 8730 Beijing 100080, People's Republic of China

and Department of Modern Physics, University of Science and Technology of China,

Hefei, Anhui 230026, People's Republic of China

(Received 26 February 1996)

The intermittent chaos in the multicomponent plasmas with negative ions has been investigated experimentally. The phenomena are modeled as a variant of classical type-I intermittency, which is studied numerically in detail. The experimental results confirmed the numerical prediction of $1/f$ noise, the probability distribution of laminar length, and the scaling law of Lyapunov exponents. A qualitative explanation on the intermittent chaos in the multicomponent plasmas with negative ions is also given. [S1063-651X(96)10608-5]

PACS number(s): 52.35.Ra, 05.45.+b

There has been a growing interest in the chaotic behavior of plasmas in the past decade. Plasma chaos is closely related with plasma turbulence, which is one of the most important problems in the field of plasma physics. Plasmas with negative ions (PNI) abound in nature and in the laboratory. A great change of the plasma characteristics is expected as a result of slightly varying the density ratio of negative ions to electrons. For example, considerable changes in the plasma properties, such as plasma structures, the stability of the discharge, and the excitation and the subsequent propagation of ion acoustic soliton, with the variation of the negative ion concentration have been observed in a wide variety of experiments. However, the nonlinear dynamics behavior in the multicomponent plasma with negative ions has not been investigated experimentally, the study of which may contribute to the understanding of its intrinsic properties and potential applications. While in nonlinear science, intermittency is well known as one of the typical routes to chaos. Since Pomeau and Manneville pioneered the analysis of intermittent transitions in the context of low-dimensional dynamical systems [1], six types of intermittencies, i.e., type I, II, III [1], X [2], V [3], and on-off [4], have been classified. All these intermittencies have been extensively observed in plasma [5–7], nonlinear oscillator [8], and various other physical systems [9]. Theoretically, each type of intermittency is studied by some general dynamical model, usually a one-dimensional restricted map of arbitrary dimension. In the type-I case, for example, the theory is developed on the quadratic map, based on which one can derive numerically or theoretically other characteristic features such as the probability distribution of laminar length, the scaling law of the average laminar length, and the Lyapunov exponent with the control parameter, $1/f$ spectrum, etc. Those derived characters are used to distinguish it from other types of intermittencies in experiments. However, other than the “classical” type-I intermittency reported in Ref. [1], there exist other varieties of type-I intermittent chaos due to different reinjection mechanisms [10,11] or high-dimension effects [12]. In these cases, the derived features such as those of the spectrum and laminar length, change greatly. In fact, the ob-

served intermittent chaos real system is much more complicated, and usually does not belong to any of the theoretical ones [13,14]. Therefore concrete analysis of the dynamical essence is strongly needed.

In this paper we report a variant of type-I intermittency observed from the multicomponent plasma with negative ions, which is classified as type I because of the tangent bifurcation mechanism behind the phenomena. It differs from others in the local shape of its dynamical map. The phenomenon is modeled and studied numerically, and the results are compared with the experimental results. We give experimental verification of the scaling laws of the Lyapunov exponent of intermittent chaos. Other features of this demonstrated intermittency include spectral structure, probability distribution of l , and a scaling relation of average laminar length $\langle l \rangle$ with ϵ , a normalized control parameter to be defined later. Most of the results agree with the numerical results.

Experiments are performed in a large multidipole steady state plasma device as described in Refs. [15,16]. The device consists of an electron-emitting cathode and current-collecting anode. The argon plasma is produced by a dc discharge between the anode and cathode. Small amounts of sulfur hexafluoride are introduced into the host Ar plasma by a piezoelectric leak valve. The electron attachment cross section of SF_6 is large at energies of the order of 1 eV so that the $Ar^+ - e^- + SF_6^-$ plasma is formed. The discharge is determined by the argon pressure (P_a), filaments current (I_f), discharge voltage (V_D), and separation between the anode and the cathode (d) and the density of negative ions ($n_{SF_6^-}$). The typical plasma parameters measured by a Langmuir probe are electron density $n_e = 10^7 - 10^8 \text{ cm}^{-3}$, electron temperature $T_e = 1 - 3 \text{ eV}$, and ion temperature $T_i \ll T_e$. Plasma space potential V_p , as monitored with an axially movable emissive probe, decreases as the amount of SF_6 is increased. The percentage of SF_6^- is estimated by monitoring the reduction of the electron saturation current of the Langmuir probe [17,18], that is, $\alpha = n_{SF_6^-} / n_{Ar^+} = 1 - I_{es} / I_{es}^0$ where I_{es} and I_{es}^0 are the elec-

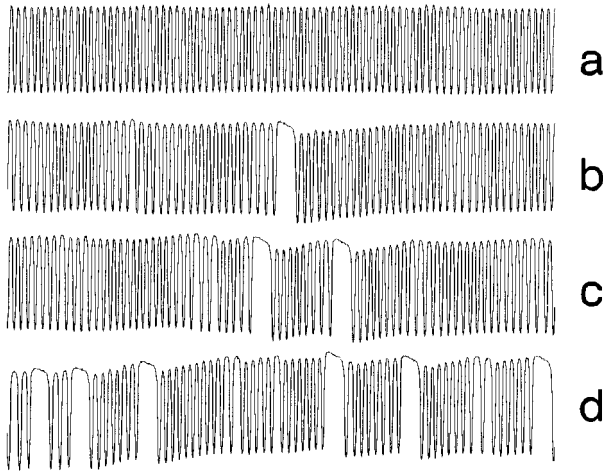


FIG. 1. Time series signals under the condition of $P_a = 8 \times 10^{-4}$ torr, $V_D = 13.00$ V, $d = 9.0$ cm, $I_f = 26$ A. (a) Stable periodic oscillation of plasma discharge current for $\epsilon = 0$. (b)–(d) Above the threshold the oscillations are interrupted by “bursts” for $\epsilon = 2.4 \times 10^{-3}$, 1.27×10^{-2} , and 1.88×10^{-2} , respectively. Arbitrary units are used for the vertical scale, and the full scale for the horizontal scale is 82 ms.

tron saturation currents of Langmuir probe with and without the SF_6^- . It is found that for the parameter range in the experiment reported here the amount of SF_6 bled into the chamber and the α value grows linearly with the voltage U applied to the piezoelectric valve. When U varies between a threshold value (≈ 90 V) and an up-limit voltage (≈ 120 V), this relation will always hold. In fact, the U value ranges only from 99 to 101 V in the experiments reported here. Therefore, instead of α , the voltage U will be used as a control parameter later in describing the experiment results. The electron saturation current $I_{es}(t)$ of the probe that is proportional to the electron density, the discharge current $I_D(t)$, and the plasma space potential V_p are recorded by digitizers (8 bits, data length 2^{16} bytes, sampling interval 16 μs).

The PNI has shown rich nonlinear dynamical phenomena that are similar to those that occur in other systems. Here we shall confine our presentation to the experimental observation of intermittent chaos in the multicomponent plasma with negative ions. Similar to previous experiments [15], we started the experiment from a pure Ar plasma, which can be controlled to approach a steady self-sustained periodic oscillation ($T_0 \approx 1$ ms, $\delta n_e/n_e \approx 10\%$) by reducing the discharge voltage V_D to the threshold value while keeping other discharge parameters (P_a, I_f, d) constant. Then, we increased gradually the amount of SF_6 fed into the Ar plasma by increasing stepwise the voltage U applied to the piezoelectric leak valve and monitored the change in the system behavior. It is observed that when U is below a critical value U_c , the regular periodic oscillation in the measured signals of I_D and I_{es} remains constant as shown in Fig. 1(a). As U is increased slightly above U_c the periodic oscillation seems to be randomly and abruptly disrupted by a short “burst.” The duration of the periodic state (so-called laminar length) is seemingly at random due to the stochastic occurrence of bursts, which leads to the mean intermittent state. The critical value

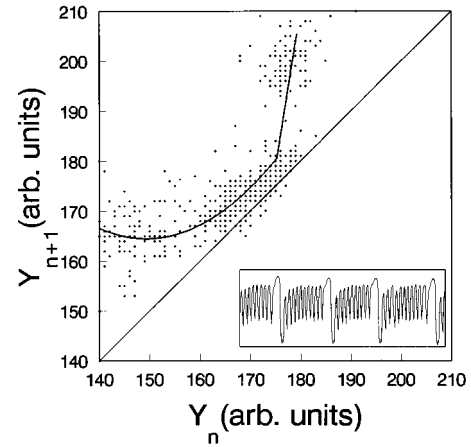


FIG. 2. Return map of $Y_{n+1} = f(Y_n)$, constructed from the plasma space potential signal (40 ms of a typical whole time series are shown in the inset) data are fitted by a quadratic curve and a line.

U_c can be estimated from the voltage U where only one burst begins to appear in a long time series signal. The normalized control parameter ϵ is defined as $(U - U_c)/U_c$. It can be seen from Figs. 1(b), 1(c), and 1(d) that the larger ϵ , the shorter the average laminar length.

The onset of intermitencies corresponds to the appearance of a new unstable direction in phase space. The correlation dimension D_2 calculated from the phase space reconstruction of time series [19] is larger than 1. To point out the dynamical properties, we construct the Poincaré return maps, which are adapted to the actual experimental situation and also constitute the framework of the theoretical model [1]. Data for the return map are obtained by taking the successive maxima of the time series of the plasma space potential signal, which are named Y_1, Y_2, \dots . Then the general discrete return maps $Y_{n+1} = f(Y_n)$ are constructed. Figure 2 shows the time series and the corresponding constructed return map with some thousands of points, many of which overlap due to the 8 bit precision. Although some scatter of the data points can be seen due to the presence of noise, the most points are located around the fitting curve consisting of a quadratic curve and a straight line, which are obtained by the least-square-fitting procedure. It can be seen that the orbits generated by the map are trapped in the narrow channel formed between the fitting curve and the identifying map. The fit yields the value of ϵ' , which is expected to be proportional to the experimental control parameter ϵ . When ϵ is gradually tuned to zero, the channel becomes narrower and finally disappears, which reveals the tangent bifurcation nature of this intermittent chaos. The overall shape of the reconstructed map is almost the same as the theoretical model map for type-I intermittency [1]. But there is a quickly expanding phase shortly after passing through the narrowest part of the channel, and then orbits enter the turbulent phase and reinject into the channel. This part of the map is different from the other part, so we use a straight line to simulate this phase. Therefore, the constructed Poincaré map does unfold the essence of the type-I intermittency of this phenomenon.

One of the remarkable statistical properties of the intermittency is the spectral power scaling law with frequency in the low-frequency region. A typical power spectrum ob-

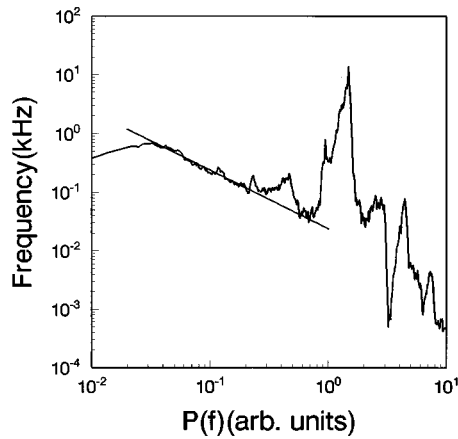


FIG. 3. The logarithm of $P(f)$ is plotted against the logarithm of the frequency for $\epsilon = 3.4 \times 10^{-3}$. The low-frequency spectrum is fitted by a line whose slope is -0.99 ± 0.02 .

tained from a time series signal for $\epsilon = 3.4 \times 10^{-3}$ near the onset of intermittency is shown as the log-log plot in Fig. 3. The spectrum associated with this intermittency is characterized by a strong enhancement of $1/f$ -type low-frequency noise with a flat plateau near to zero frequency, in addition to a broad peak at $f \approx 1$ kHz. The low-frequency noise is found to have a power-law spectrum $f^{-\delta}$ with exponent $\delta = 0.99 \pm 0.02$ in the frequency range of $0.03 < f < 0.7$ kHz. This is consistent with the theoretical results for the type-I intermittent chaos where an inverse power law $1/f$ of the power spectrum is observed [20]. The stochastic distribution of laminar length contributes to the major part of the low-frequency noise. The flat plateau stems from perturbations by external noise that cause arbitrarily long laminar periods to become finite.

In order to reveal the properties of this kind of intermittency, we constructed a model map in reference to the fitting curve of Fig. 2, as shown in Fig. 4(a), where another straight line is added to the constructed map to provide a reinjecting

mechanism. The data generated from the map can simulate the overall shape of the real time series; thus it can be used to obtain the power spectrum of the data by the fast Fourier transform algorithm. The corresponding spectrum of the map is plotted as curve (1) in Fig. 4(b). The low-frequency spectrum diverges with the scale as $f^{-(0.95 \pm 0.05)}$ over two decades in frequency f and reaches a plateau that is due to the non-existence of arbitrary long laminar length and the limited data length of the time series. Noise always exists in most physical experimental systems and sometimes it will affect some properties of the system dramatically. Therefore, in order to compare the results from the model map with that of experiments more practically, noise is introduced to the model map in Fig. 4(a). The new noisy map takes the form

$$Y_{n+1} = M(Y_n) + \xi,$$

where M is the noise free model map, and ξ is a small amplitude Gaussian noise. It is observed that the low-frequency plateau width of the spectrum increases with increasing noise level, a similar case of which has also been observed in the numerical simulation of chaos-chaos intermittency in Chua's circuit by Anishchenko, Nieman, and Chua [21]. Two of the spectra computed from this noisy map are shown in Fig. 4(b), curves (2) and (3), corresponding to noise-to-signal ratios of 0.3% and 1.0%, respectively. One can easily find that only 1.0% Gaussian noise can make the dynamic range of $1/f$ noise part of the spectrum decrease from over two decades to only about one decade. This result conforms to experiment, and points out again the manifold intermittent chaos in real physical systems. Furthermore, we compute the Lyapunov exponent λ and average laminar length $\langle l \rangle$ for different values of ϵ' from the model map. The numerical results show $\lambda \propto \epsilon'^{0.50}$ and $\langle l \rangle \propto \epsilon'^{-0.55}$. These two scaling laws are almost the same as that of the classical type-I intermittency. The probability distribution of laminar length $P(l)$ is also obtained numerically; its shape is similar to that of the classical one.

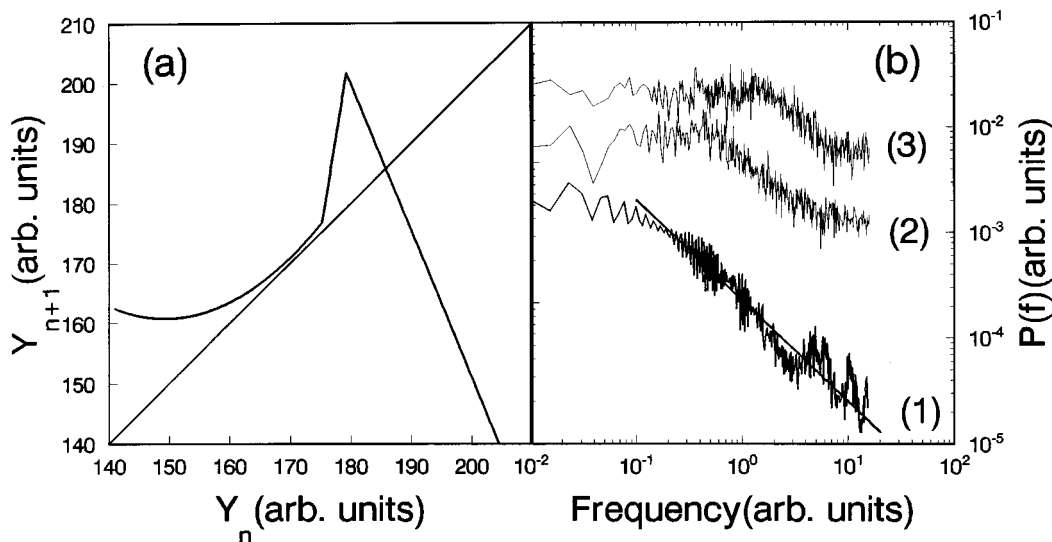


FIG. 4. Model map (a) and the corresponding spectra (b). The spectra labeled (1), (2), and (3) in (b) correspond to the map without and with 0.3% and 1.0% Gaussian noise. The fitting line in (b) has the slopes of -0.95 .

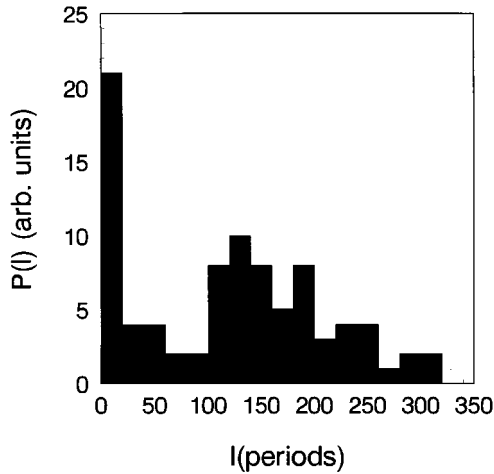


FIG. 5. Histogram of the probability distribution $P(l)$ of laminar length l at $\epsilon = 5.5 \times 10^{-3}$.

In the following context, we return to experiments to see if the intermittent chaos observed in our experiments can behave like that obtained from the model map. One of the experimentally measurable characteristics of the intermittency is the probability distribution $P(l)$ of laminar length. The probability distribution $P(l)$ of laminar length for a given $\epsilon = 5.5 \times 10^{-3}$ is plotted as the histogram versus l in Fig. 5. Although the statistics of the distribution is not good enough due to the finite sampling duration of the experiments, it still can be seen clearly that after an initial decay there is a hump at $l = 150$ with a large tail at large values of l . This is similar to the numerical simulations of intermittent chaos from the model map with the presence of external noise and the numerical results computed by Hirsh, Huberman, and Scalapino [22]. Therefore this laminar length distribution may be explained by the presence of noise or other spurious signals in our experiments.

Furthermore, the scaling law of Lyapunov exponent and average laminar length on ϵ play an important role in classifying types of intermittent chaos. The existence of scaling law, just as the theory of phase transition, results in a great economy in dealing with data and provides the framework for distinguishing the intrinsic chaotic behavior from the fluctuations induced by the external noise. However, for a given unknown dynamical system it is very difficult to extract the scaling law of laminar length accurately from experimental signals, except for a few electric circuit experiments. The major reason for this difficulty is that in the analysis of experimental data the statistics becomes poor for longer laminar length at small ϵ due to limited data length, and the boundary between the laminar and burst becomes obscure and the effects of noise on the measurement of laminar length become important for shorter laminar length at large ϵ . In fact the scaling law of the average laminar length and the Lyapunov exponent characterize the intermittent process in different respects. The average laminar length $\langle l \rangle$ measures the time scale of the correlation of intermittency. A dynamical system becomes more chaotic with decreasing correlation. On the other hand, a positive Lyapunov exponent is the average exponential rate of divergence of nearby orbits in phase space in time; the reciprocal of Lyapunov

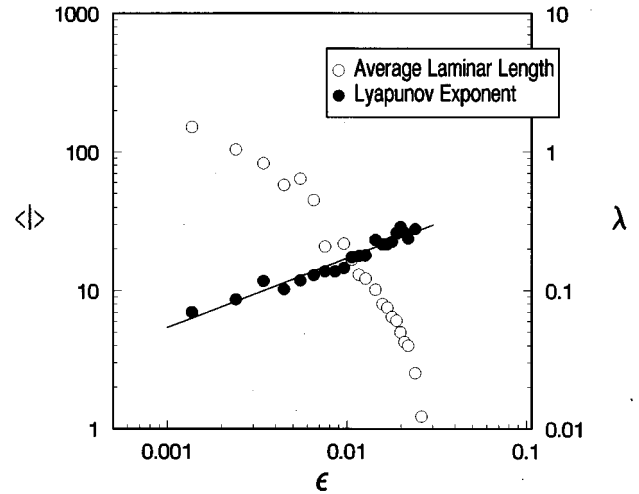


FIG. 6. Plot of $\log_{10}(\lambda_1)$ vs $\log_{10}(\epsilon)$ (solid dots). The $1/2$ power law is fair held. But the $\log_{10}\langle l \rangle$ vs $\log_{10}(\epsilon)$ (circles) has not such a linear relation.

exponent shows the predictable time scale of a dynamical system. For intermittent chaos, the scaling law of the Lyapunov exponent describes the stability losing rate of the system with the change of the channel width, or the distance from the bifurcation point. This is a very important statistical property of the intermittent chaotic system. The Lyapunov exponents are calculated with the help of a phase space reconstruction technique [15,19] from time series signals. Before applying the algorithm to the experimental intermittent chaos signal, we verified this algorithm with the intermittent chaotic attractor of Lorentz equations and got the $\lambda \sim \epsilon^{1/2}$ scaling law, which proves its applicability in the intermittency case. For the experimental data, the dependence of λ on ϵ in the range of $\epsilon = 1.0 \times 10^{-3}$ through 2×10^{-2} is plotted in Fig. 6. The portrait of the $\log_{10}(\lambda_1) \sim \log_{10}(\epsilon)$ shows the slope of the straight line of the fit data is 0.52. From other similar runs, the average value of the slope is found to be 0.52 ± 0.04 . That is, the leading Lyapunov exponent grows with $1/2$ power, which agrees with the numerical prediction. Our algorithm [15,19] for the calculation of the Lyapunov exponent from the experimental data is insensitive to the presence of noise while the noise amplitude is less than 10%. Therefore this enables us to get a relatively accurate scaling law of the Lyapunov exponent on ϵ . However, due to poor statistics, poor experimental resolution of laminar length, and unavoidable noise, from experimental data we cannot get a scaling law of laminar length on ϵ that agrees with the numerical prediction. In the experiments the presence of noise makes the average laminar length become shorter than in the absence of noise. The poor resolution of laminar length also results in the shorter computing laminar length. Therefore, as for the scaling law of laminar length, which is also shown in Fig. 6, there does not exist a simple linear relation between $\log\langle l \rangle$ and $\log\epsilon$.

In summary we have observed a variant of type-I intermittent chaos in a multicomponent plasma with negative ions. This intermittent behavior is reversible when the density of $n_{SF_6^-}$ is varied, and then the approach to the chaotic state is continuous. We believe that a clear experimental confirmation of a type-I like intermittent route in the multicom-

ponent plasmas has been obtained by return map, $1/f$ noise, probability distribution of the laminar length, and especially the scaling law of the leading Lyapunov exponent λ_1 on the control parameter. A self-sustained periodic oscillation is thought to be related to a moving double layer as demonstrated by particle simulation [23] and our recent experiments where we found that the velocity of a weak moving double layer is $(0.5 - 1) \times 10^5$ cm/s. The production of negative ions can cause the reduction of cathode fall, which strongly influences these primary emissive electrons from the cathode. The periodic oscillation of discharge current, quite sensitive to the primary emissive electrons, is interrupted by the appearance of negative ions, which reduces plasma density. On the other hand the production of negative ions also relies on electron density. The decrease of electron density causes the reduction of negative ions, then the cathode

sheath recovers and the plasma density increases. This process repeats. There exists a feedback mechanism between the appearance and disappearance of negative ions, which may correspond to the relaminarization mechanism mathematically. Anyway a complete explanation of dynamics behavior could not be given at present. Nevertheless, the experimental observation presented may help in the development of models for the variety of behavior in the multicomponent plasma with negative ions.

The authors wish to thank Professor Y. Gu and B.H. Wang for fruitful and interesting discussions. This work is supported by Doctoral Training Foundation of National Education Commission, Huo Yindong Education Foundation and National Basic Research Project "Nonlinear Science."

-
- [1] Y. Pomeau and P. Manneville, *Commun. Math. Phys.* **74**, 189 (1980).
- [2] T.J. Price and T. Mullin, *Physica D* **48**, 29 (1991).
- [3] M. Bauer, S. Habip, D.R. He, and W. Martienssen, *Phys. Rev. Lett.* **68**, 1625 (1992).
- [4] N. Platt, E.A. Spiegel, and C. Tresser, *Phys. Rev. Lett.* **70**, 279 (1993).
- [5] P.Y. Cheung, S. Donovan, and A.Y. Wong, *Phys. Rev. Lett.* **61**, 1360 (1988).
- [6] Jiang Yong, Wang Haida, and Yu Changxuan, *Chin. Phys. Lett.* **5**, 489 (1988).
- [7] J. Qin, L. Wang, D.P. Yuan, P. Gao, and B.Z. Zhang, *Phys. Rev. Lett.* **63**, 163 (1989).
- [8] Carson Jeffries and Jose Perez, *Phys. Rev. A* **26**, 2117 (1982); Jung-yn Huang and Jong-Jean Kim, *ibid.* **36**, 1495 (1987); P. Richetti, F. Argoul, and A. Arneod, *ibid.* **34**, 726 (1986).
- [9] Y. Pomeau, J.C. Roux, A. Rossi, S. Bachelart, and C. Vidal, *J. Phys. (Paris) Lett.* **42**, 271 (1981); M. Dubois, M. A. Rubio, and P. Berge, *Phys. Rev. Lett.* **51**, 1446 (1983).
- [10] Chil-Min Kim, O.J. Kwon, Eok-Kyun Lee, and Hoyun Lee, *Phys. Rev. Lett.* **73**, 525 (1994).
- [11] Byon Chol So and Hazime Mori, *Physica* **21D**, 126 (1986).
- [12] Harvey Kaplan, *Phys. Rev. Lett.* **68**, 553 (1992).
- [13] G. Baier, K. Wegmann, and J.L. Hudson, *Phys. Lett. A* **141**, 340 (1989).
- [14] A. Komori, N. Ohno, T. Yamaura, and Y. Kawai, *Phys. Lett. A* **170**, 439 (1992).
- [15] Ding Weixing, Huang Wei, Wang Xiaodong, and C.X. Yu, *Phys. Rev. Lett.* **70**, 170 (1993).
- [16] W.X. Ding, H.Q. She, W. Huang, and C.X. Yu, *Phys. Rev. Lett.* **72**, 96 (1994).
- [17] H. Amemiya, *J. Phys. D* **23**, 999 (1990).
- [18] Jamie L. Cooney, Matthew T. Gravin, and Karl E. Lonngren, *Phys. Fluids B* **3**, 2758 (1991).
- [19] W. Huang, W.X. Ding, D.L. Feng, and C.X. Yu, *Phys. Rev. E* **50**, 1062 (1994).
- [20] H. Mori, H. Okamoto, B.C. So, and S. Kuroki, *Prog. Theor. Phys.* **76**, 784 (1986).
- [21] V.S. Anishchenko, A.B. Neiman, and L.O. Chua, *Int. J. Bifur. Chaos* **4**, No. 1, 99 (1994).
- [22] J.E. Hirsch, B.A. Huberman, and D.J. Scalapino, *Phys. Rev. A* **25**, 519 (1982).
- [23] F. Greiner, T. Klinger, H. Klostermann, and A. Piel, *Phys. Rev. Lett.* **70**, 3071 (1993).